Crystal-state–amorphous-state transition in low-temperature silicon homoepitaxy

M. V. Ramana Murty and Harry A. Atwater
Thomas J. Watson Laboratories of Applied Physics, California Institute of Technology, Pasadena, California 91125
(Received 23 August 1993)

Conventional molecular-beam epitaxy of Si(001) at low temperatures proceeds epitaxially up to a finite thickness followed by a crystalline-to-amorphous transition. Concurrent low-energy Ar^+ ion irradiation during deposition results in an increase in epitaxial thickness. Surface smoothing is shown to be the primary effect of Ar^+ ion irradiation. A possible pathway to the formation of amorphous silicon is the nucleation of twin boundaries on {111} planes. The intersection of a twin boundary with other {111} or {001} planes results in the formation of five- and seven-member rings which leads to the crystalline-to-amorphous transition.

The extension of silicon homoepitaxy to lower temperatures is both of fundamental and technological interest. Low-temperature growth of Si on Si(001) proceeds epitaxially up to a finite thickness followed by a crystalline-to-amorphous transition.[1] This breakdown of epitaxy has been observed in a number of other systems, including Si on Si(111) (Ref. 2) and GaAs on GaAs(001).[3] An elemental semiconductor such as Si(001) with a relatively simple reconstruction provides an ideal system for the investigation of this transition. A variety of energetic beam techniques such as sputter deposition,[4] direct ion-beam deposition,[5] and ion-beam-assisted molecular-beam epitaxy (IAMBE) (Ref. 6) have been successfully employed to extend the growth of defect-free crystalline silicon at low temperatures. Despite all these advances, the cause of the transition to deposition of amorphous silicon is not known. In this Brief Report, we describe the structure and the nature of defects in low-temperature Si films. We consider the possible role of impurities, especially hydrogen, and the influence of surface roughness on the crystalline-to-amorphous transition. A pathway to the nucleation of amorphous silicon through the formation of twin boundaries on {111} planes is discussed.

Si(001) wafers were cleaned using standard wet chemical techniques,[7] and terminated with a dihydride surface by a 50-s dip in dilute HF solution (5% HF in H_2O) before transfer to the ultrahigh vacuum deposition chamber. The details of the deposition system are described elsewhere.[6] Silicon films were deposited using an electron gun, and a Kaufman source was used to generate Ar^+ ions. Films were analyzed *in situ* by reflection high-energy electron diffraction (RHEED) and *ex situ* by transmission electron microscopy (TEM), atomic force microscopy (AFM), secondary-ion-mass spectrometry (SIMS), and Rutherford backscattering/channeling.

A TEM image of a 220-nm film deposited at 370 °C by conventional molecular-beam epitaxy (MBE) is shown in Fig. 1(a). The growth rate was 0.09 nm/s. The film is epitaxial up to a thickness of about 83 nm, following which defects with increasing density are observed. Further growth results in a complete transformation to amorphous film deposition. One measure of the quality of the epitaxial film is the epitaxial thickness h_{epi}. We take the thickness up to which the film is defect free in a TEM image as our definition of h_{epi}. This is justified by the high density of nucleation sites of amorphous Si within the limited region observable by cross-section TEM. The presence of twins can be inferred from the moiré fringes with a period of three {111} lattice plane spacings. Other defects observed in the region include stacking faults and "hydrogen platelets." A through-focus series showed

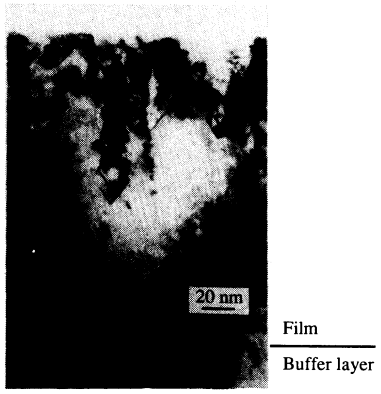

(a)

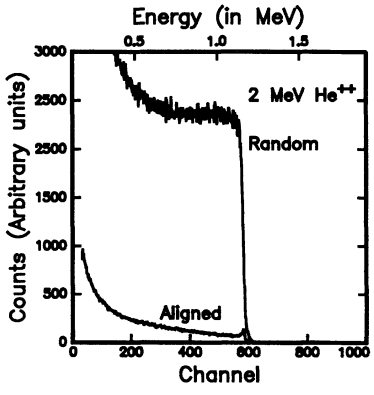

(b)

FIG. 1. (a) Bright field TEM image of a 220-nm film deposited at 370 °C by conventional MBE, imaged in the ⟨110⟩ projection under multibeam conditions. (b) A channeling spectrum from a 50-nm film deposited under conditions identical to (a), giving $\chi_{min}=0.03$. It is noted that about 75% of the signal from the film falls within the surface peak.

that some of the defects do not show the contrast of a stacking fault or a dislocation. The defect contrast is similar to the "hydrogen platelets" reported in hydrogen plasma etching of silicon.[8] Figure 1(b) shows a channeling spectrum from a 50-nm film deposited under identical conditions. The minimum yield χ_{min} of 0.03 indicates a film with a low defect density. Plan-view TEM analysis showed no defects in a 100-μm^2 area of the sample, giving a defect density of less than 10^6 cm^{-2}. This establishes the abrupt and local nature of the breakdown of epitaxy. IAMBE films were deposited with 50-eV Ar^+ ions and an ion-to-atom flux ratio of approximately 0.06. The ions were incident at 45° to the surface normal. An IAMBE film deposited at 370°C with a growth rate of 0.09 nm/s showed an increased epitaxial thickness h_{epi} of 130 nm. A channeling spectrum from an 80-nm film grown under identical conditions also gave a χ_{min} value of 0.03, indicating a film with a low defect density.

The most common components of the residual gas during deposition are C, H, and O containing species such as atomic H and O, H_2, CO, H_2O, CO_2, and CH_x. Figure 2 shows the SIMS profile of carbon and oxygen in the films deposited by conventional MBE and IAMBE described above. A relatively high base pressure of 10^{-6} Pa in the SIMS analysis chamber limited the sensitivity of the method. The background levels of H and O in Fig. 2(a) are about 2×10^{19} cm^{-3} and 1×10^{19} cm^{-3}, respectively. The two peaks in the C and O profiles correspond to the film–buffer-layer and the buffer-layer–substrate interface. In the conventional MBE film, about 0.005 monolayer (ML) of C and 0.02 ML of O was accumulated in the elapsed time between buffer layer growth and commencement of low-temperature growth. This layer of impurities gives rise to the contrast at the interface in TEM cross section images. In the IAMBE film, C and O concentrations in the low-temperature film are higher compared to the buffer layer. This is believed to be due to contaminants in the ion beam. The rise in C and O concentrations toward the surface coincides with the observation of defects in the film. Carbon or oxygen contamination, however, is unlikely to be the cause of breakdown of epitaxy. This is seen from an annealing experiment first reported in Ref. 1. It is found that by repeating the cycle of (a) deposition up to h_{epi} at the low temperature, and (b) a 1-min anneal (no film growth) at $T_A = 500$ °C, one can grow crystalline silicon indefinitely. We found that a 10-min anneal at 450 °C produces the same effect. The annealing temperature T_A, however, is too low for desorption of either C or O, and indeed the ability to grow thick single-crystal silicon layers at 500 °C gives further support to this conclusion. Amorphous silicon has a high density of dangling bonds, which gives rise to the high C and O concentrations observed near the surface in Fig. 2 once amorphous Si deposition has begun. Alternatively, C and O could have diffused into amorphous silicon after exposure to atmosphere. The annealing temperature T_A is sufficiently high to desorb hydrogen. Observation of a RHEED pattern during the annealing revealed a remarkable smoothing of the surface. We now turn to these two aspects, namely hydrogen contamination and surface roughness.

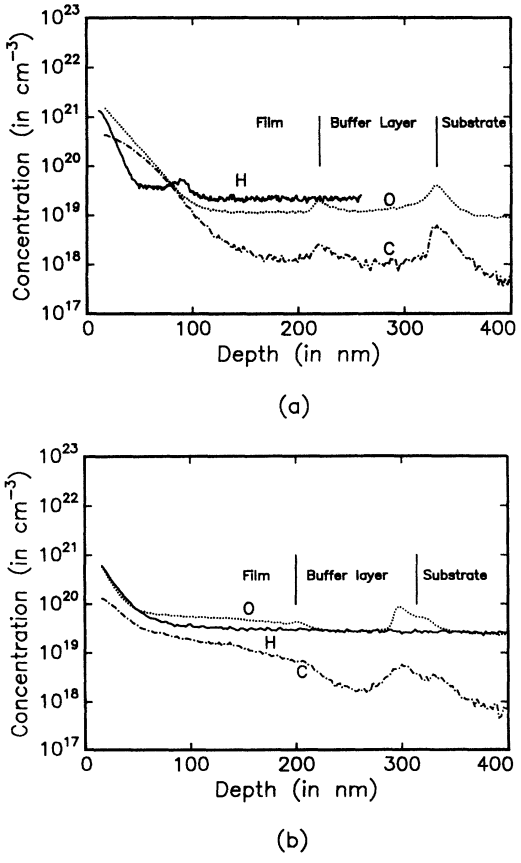

FIG. 2. SIMS depth profiles of carbon, oxygen, and hydrogen from (a) a conventional MBE and (b) an IAMBE film. C and O profiles were obtained with a 10.5-keV Cs^+ beam; the H profile was obtained with a 14.5-keV O_2^+ beam. A relatively high base pressure of 10^{-6} Pa in the SIMS analysis chamber limited the H and O sensitivity. Note that the background levels of H and O are different for (a) and (b).

Hydrogen adsorption on Si(001) at room temperature results in a (1×1) dihydride-terminated surface. The surface transforms to a (2×1) reconstructed monohydride following partial hydrogen desorption at 350–400 °C, and complete hydrogen desorption occurs at 450–500 °C.[9] Conventional MBE on an initially dihydride surface results in an amorphous film as shown in Fig. 3(a). Epitaxial growth has been reported at 370 °C on an initially monohydride surface with a thermal Si beam[10] and at 210 °C on an initially dihydride surface with an energetic Si beam.[4] A SIMS profile of hydrogen

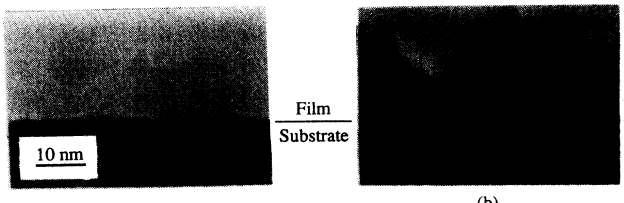

FIG. 3. (a) High-resolution cross-section TEM image of amorphous film growth on an initially dihydride surface at 190 °C. (b) Film growth proceeds epitaxially on a similar surface following Ar^+ ion beam-induced reconstruction at 190 °C.

is shown in Fig. 2. We see a high concentration toward the surface, and this is a result of the high density of dangling bonds in amorphous silicon and the formation of platelet defects. Hydrogen platelet defects have been reported to cause a lattice dilation of 20–30%.[8] It was found that 50-eV Ar^+ ion irradiation (incidence angle 65° with respect to the surface normal) at 100 °C on an initially dihydride-terminated Si(001)-1×1 surface results in a reconstructed Si(001)-2×1 surface. Growth on such substrates proceeds epitaxially; an example of a substrate prepared at 190 °C is shown in Fig. 3(b). Low-energy Ar^+ ion irradiation can thus sputter hydrogen from the surface.

Silicon film growth at low temperatures proceeds by formation of three-dimensional islands. Both {111} and {311} facets are observable at the growing front in TEM images.[6] The evolution of surface morphology was studied by atomic force microscopy. AFM was performed *ex situ* and the samples were dipped in dilute HF just prior to imaging. Films of different thicknesses were deposited side by side at 240 and 325 °C by conventional MBE. The growth rate was 0.09 nm/s. The images obtained from the films at 325 °C are shown in Figs. 4(a)–4(d). Island coalescence and an increase in surface roughness with film thickness can be readily inferred from the images. IAMBE films were also deposited at 325 °C and 0.09 nm/s using 50-eV Ar^+ ions. These films were deposited separately, as it was not possible to simultaneously block the ion and growth fluxes in different regions. As a consequence, some sample variation is expected. Figure 4(e) shows the surface of an IAMBE film after 40-nm deposition. Comparison with Fig. 4(b) clearly shows that Ar^+-ion bombardment leads to surface smoothing. The epitaxial thicknesses are estimated to be 20 and 50 nm at 240 and 325 °C, respectively, for the conventional MBE films, and 140 nm for the IAMBE film. The rms surface roughness R_q was measured over a 300×300-nm^2 region at three separate points on each specimen, and is shown as a function of film thickness in Fig. 5. We see that R_q at the breakdown of epitaxy is different for different growth conditions. This shows that rms surface roughness is not a global parameter for describing the breakdown of epitaxy.

Based on the above results, we can make some observations regarding the influence of various parameters on the crystal-to-amorphous transition. One possible viewpoint is that hydrogen alone is responsible for this transition. Hydrogen atoms could saturate the bonds of silicon surface atoms, leaving the incoming Si atoms without a lattice to conform to. Indeed, conventional MBE on a dihydride surface results in an amorphous layer. However, there is a difficulty with this viewpoint because hydrogen desorption is negligible below 350 °C on the time scale of film growth; but h_{epi} is observed to exhibit a strong dependence on temperature.[1,6] Consider roughness alone as a cause of breakdown of epitaxy. Surface roughness has a positive correlation with the temperature dependence of h_{epi}. We have also observed that concurrent low-energy Ar^+-ion irradiation during deposition results in surface smoothing. It is plausible to speculate that

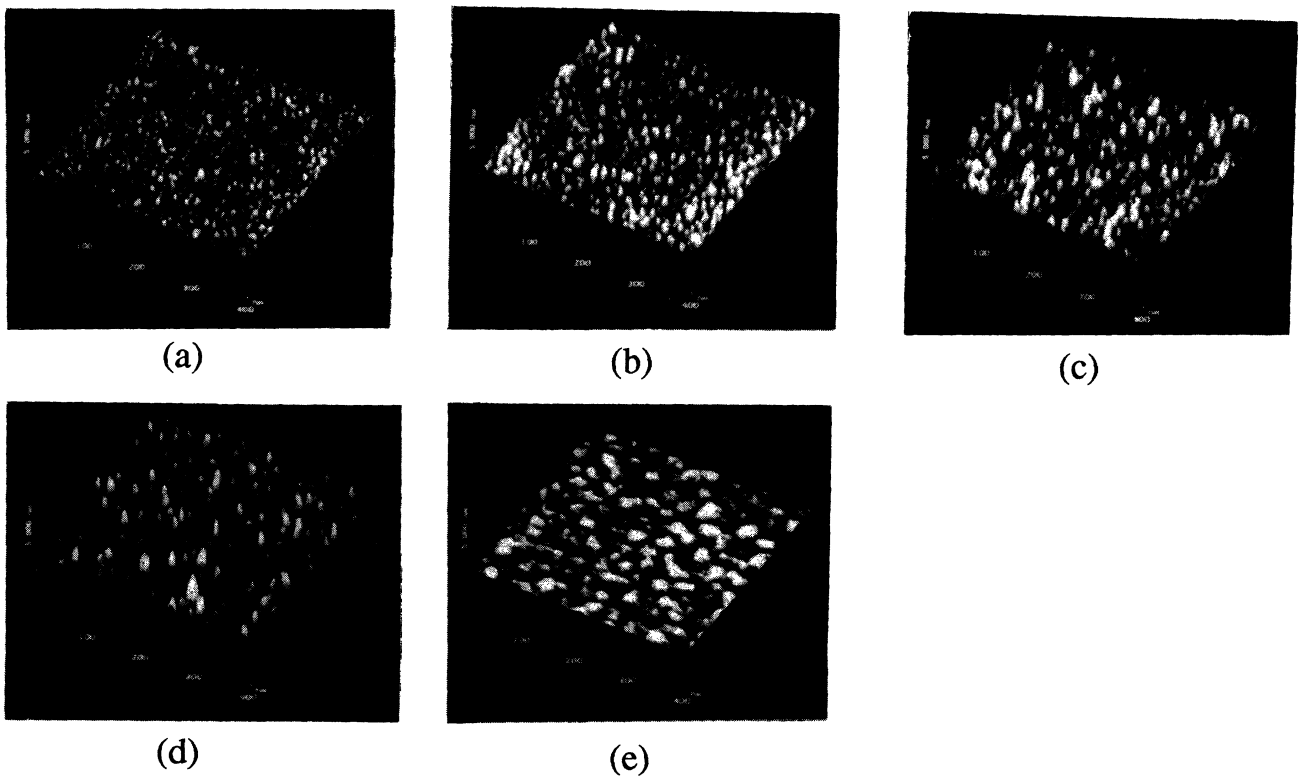

FIG. 4. AFM images after (a) 20-, (b) 40-, (c) 60-, and (d) 80-nm film deposited at 325 °C. The growth rate was 0.09 nm/s. (e) AFM image of an IAMBE film after 40-nm deposition at 325 °C. 50-eV Ar^+ ions and an ion-to-atom flux ratio of about 0.06 were used. The horizontal and vertical scales are 100 nm/division and 2.5 nm/division, respectively.

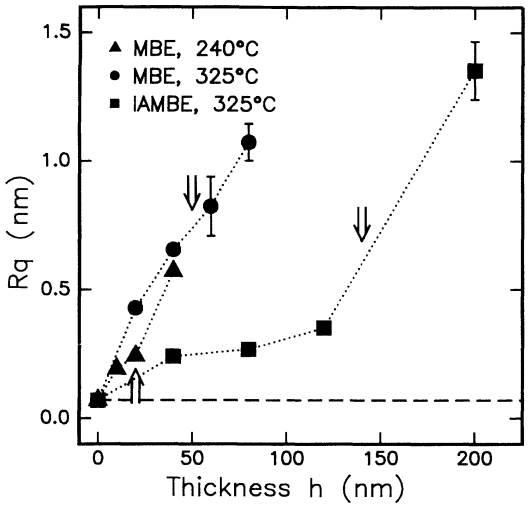

FIG. 5. The rms surface roughness R_q vs film thickness for different growth conditions. The roughness was measured over a 300×300-nm^2 region at three separate points for each film thickness. Conventional MBE at (a) ♦, 240 °C and (b) ●, 325 °C, and IAMBE at (c) ■, 325 °C. The arrows indicate the approximate epitaxial thickness. The dashed line is the measured roughness of a high-temperature buffer layer.

amorphous silicon nucleates at a nonplanar crystallographic feature such as a reentrant corner on the surface. It is noted that the h_{epi} values reported by different groups[1,6,11] differ by an order of magnitude for similar growth conditions. The presence of microvoids, or volume defects, has been mentioned as a cause of breakdown of epitaxy.[11,12] In our experiments, the crystalline-to-amorphous transition was observed to occur without microvoids. This agrees with the results of Ref. 13, where the point defect density in the crystalline layer was shown to be too low to account for the crystalline-to-amorphous transition. Finally, another viewpoint is that a combination of hydrogen adsorption and increase in surface roughness lead to the breakdown of epitaxy. The formation of hydrogen platelets on {111} planes and the smoothing of the surface in the annealing experiment described above support this notion.

A possible pathway to the nucleation of amorphous silicon could be as follows. The continuous random network models of amorphous silicon show that besides six-member rings, it consists of five- and seven-member rings. At low temperatures, growth on Si(001) surfaces leads to an increase in surface roughness and the formation of {111} facets. Due to the lower diffusivity of Si adatoms at low temperatures, twin boundaries can form on such planes as they cost relatively little energy. When a twin boundary formed on one particular {111} plane meets other {111} or {001} planes, it inevitably leads to the formation of five- and seven-member rings. At very low temperatures ($T \lesssim 150$ °C) this rapidly leads to a transformation to amorphous film deposition. At more moderate temperatures ($150 \lesssim T \lesssim 450$ °C), a crystalline film continues to grow after the formation of a grain boundary because a crystalline network with defects still has lower energy than an amorphous network. Eventually the density of the defects grows very high, leading to a transition to amorphous silicon deposition. In fact, molecular-dynamics simulations of epitaxy on Si(111) have shown that the breakdown of epitaxy occurs at the edge of a stacking fault.[2] The role of impurities could simply be to accelerate the roughness of the film by tying up growth sites.

In conclusion, we have observed that concurrent low-energy Ar^+-ion irradiation during Si molecular-beam epitaxy results in both hydrogen desorption and surface smoothing. Observations of the hydrogen sputtering rate are consistent with the notion that surface smoothing is the more important effect of low-energy Ar^+-ion bombardment on the crystal-to-amorphous transition. Epitaxy is possible at temperatures as low as 100 °C on substrates prepared by Ar^+-ion-beam-induced reconstruction. A pathway to the formation of amorphous silicon could be the nucleation of twin boundaries on {111} planes. The intersection of the twin with other {111} or {001} planes results in the formation of five- and seven-member rings which leads to the crystalline-to-amorphous transition.

We would like to thank C. Garland, I. Hutcheon, M. Easterbrook, and J. H. Nagel for help with TEM observations, SIMS analysis, Rutherford backscattering (RBS) analysis, and AFM observations, respectively. This work was supported by the NSF under Grant No. DMR 8958070, and by IBM.

[1]D. J. Eaglesham, H.-J. Gossmann, and M. Cerullo, Phys. Rev. Lett. **65**, 1227 (1990).
[2]B. E. Weir, B. S. Freer, R. L. Headrick, D. J. Eaglesham, G. H. Gilmer, J. Bevk, and L. C. Feldman, Appl. Phys. Lett. **59**, 204 (1991).
[3]Z. Liliental-Weber, W. Swider, K. M. Yu, J. Kortright, F. W. Smith, and A. R. Calawa, Appl. Phys. Lett. **58**, 2153 (1991).
[4]D. L. Smith, C.-C. Chen, G. B. Anderson, and S. B. Hagstrom, Appl. Phys. Lett. **62**, 570 (1993).
[5]K. G. Orrman-Rossiter, A. H. Al Bayati, D. G. Armour, S. E. Donnelly, and J. A. van den Berg, Nucl. Instrum. Methods B **59**, 197 (1991).
[6]M. V. R. Murty, H. A. Atwater, A. J. Kellock, and J. E. E. Baglin, Appl. Phys. Lett. **62**, 2566 (1993).
[7]A. Ishizaka and Y. Shiraki, J. Electrochem. Soc. **133**, 666 (1986).
[8]N. M. Johnson, C. Doland, F. Ponce, J. Walker, and G. Anderson, Physica B **170**, 3 (1991).
[9]G. Shulze and M. Henzler, Surf. Sci. **124**, 336 (1983).
[10]D. J. Eaglesham, G. S. Higashi, and M. Cerullo, Appl. Phys. Lett. **59**, 685 (1991).
[11]D. D. Perovic, G. C. Weatherly, P. J. Simpson, P. J. Schultz, T. E. Jackman, G. C. Aers, J. P. Noël, and D. C. Houghton, Phys. Rev. B **43**, 4257 (1991).
[12]H. Schut, A. Vanveen, G. F. A. Vandewalle, and A. A. Vangorkum, J. Appl. Phys. **70**, 3003 (1991).
[13]H.-J. Gossmann, P. Asokakumar, T. C. Leung, B. Nielsen, K. G. Lynn, F. C. Unerwald, and L. C. Feldman, Appl. Phys. Lett. **61**, 540 (1992).

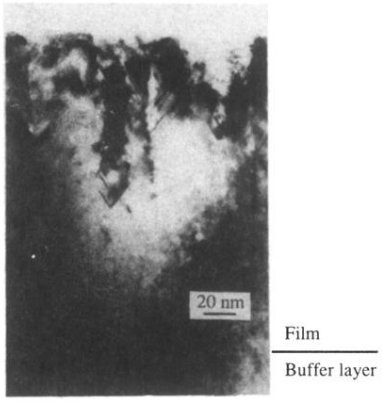

(a)

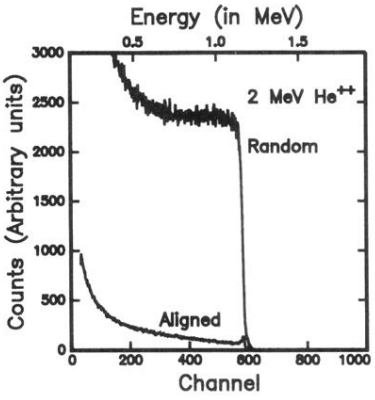

(b)

FIG. 1. (a) Bright field TEM image of a 220-nm film deposited at 370 °C by conventional MBE, imaged in the ⟨110⟩ projection under multibeam conditions. (b) A channeling spectrum from a 50-nm film deposited under conditions identical to (a), giving $\chi_{min}=0.03$. It is noted that about 75% of the signal from the film falls within the surface peak.

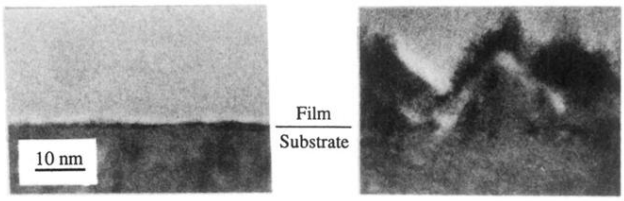

FIG. 3. (a) High-resolution cross-section TEM image of amorphous film growth on an initially dihydride surface at 190 °C. (b) Film growth proceeds epitaxially on a similar surface following Ar^+ ion beam-induced reconstruction at 190 °C.

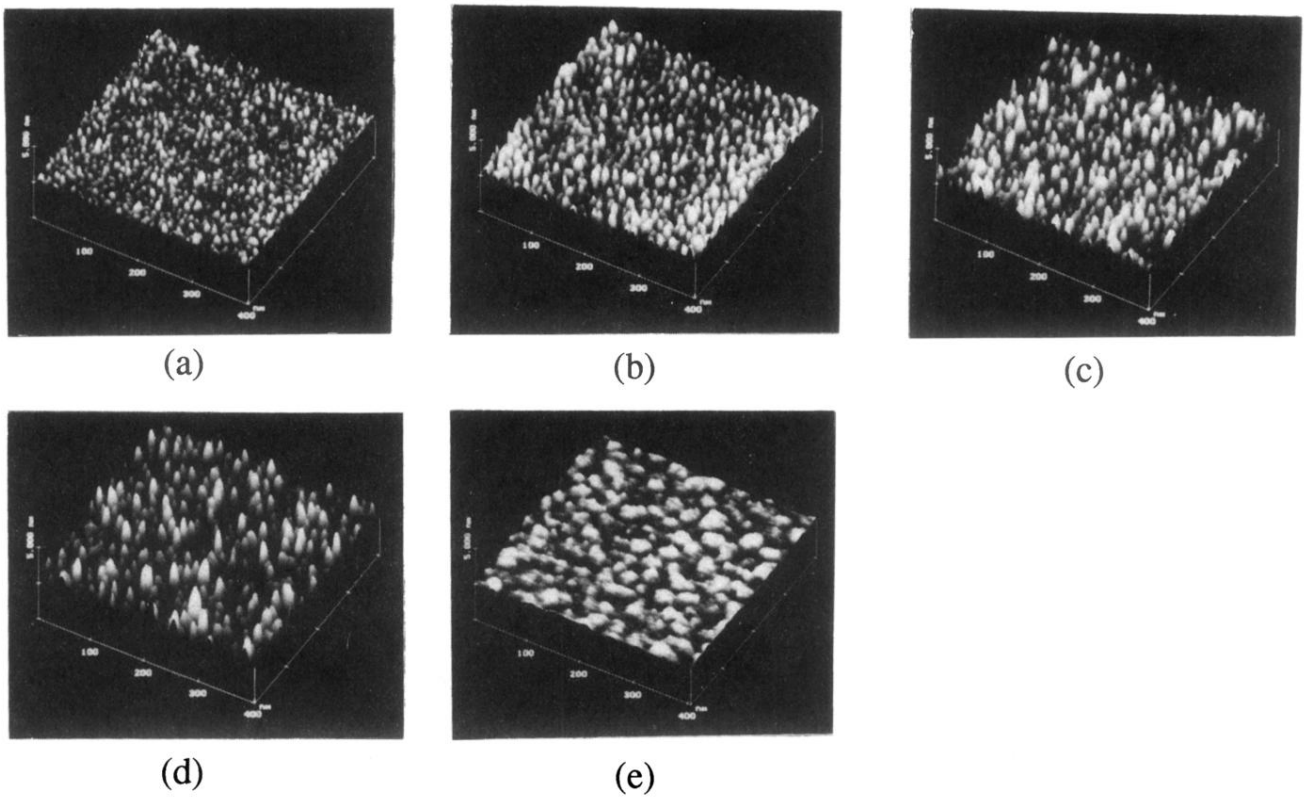

FIG. 4. AFM images after (a) 20-, (b) 40-, (c) 60-, and (d) 80-nm film deposited at 325 °C. The growth rate was 0.09 nm/s. (e) AFM image of an IAMBE film after 40-nm deposition at 325 °C. 50-eV Ar^+ ions and an ion-to-atom flux ratio of about 0.06 were used. The horizontal and vertical scales are 100 nm/division and 2.5 nm/division, respectively.